International Journal of Current Science Research and Review
ISSN: 2581-8341
Volume 07 Issue 10 October 2024
DOI: 10.47191/ijcsrr/V7-i10-20, Impact Factor: 7.943
IJCSRR @ 2024
www.ijcsrr.org

A Clinical and Radiographical Study on Augmentation of Fracture Healing in Long Bones of Dogs Using Synthetic Nanohydroxyapatite

E Sony Sharlet[1], S Bharathi*[2], R V Suresh kumar[3], M Santhilakshmi[4]

[1] PG Scholar, Dept of Surgery and Radiology, College of Veterinary Science, SVVU, Tirupati, Andhra Pradesh, India – 517 502

[*2] Professor, VSR, Dept of Veterinary Clinical Complex, College of Veterinary Science, SVVU, Tirupati, Andhra Pradesh, India – 517 502

[3]Professsor and Univ. Head, Dept of Surgery and Radiology, College of Veterinary Science, SVVU, Tirupati, Andhra Pradesh, India – 517 502

[4] Professor, Dept of Anatomy, College of Veterinary Science, SVVU, Tirupati, Andhra Pradesh, India – 517 502

ABSTRACT: Long bone fractures in six dogs were stabilized with intramedullary pinning and synthetic nanohydroxyapatite (Nha) graft material was deposited at the fracture site intra-operatively. The fractures were classified according to AO ASIF method of classification and the outcome of open reduction and internal fixation was evaluated based on clinical and radiological studies, on 7th, 15th, 30th and 45th post- operative days. Post-operative weight bearing and angulation and lameness grading, radiographic evaluation for alignment and implant stability were also evaluated. The stabilization technique proved to be satisfactory in all the cases. The radiographic score indicated better long bone fracture healing with Nha alone as a graft.

KEYWORDS: Dog, Long bone fracture, Nanohydroxyapatite

I. INTRODUCTION

Fracture of long bone is a commonly encountered orthopaedic problem in canine surgery. Most of the canine long bone fractures occur either as a result of falling from the height or from trauma sustained by automobile accidents. (Kumar *et al*., 2007; Kushwaha *et al*., 2011; Simon *et al*., 2011; Ali, 2013, Sirin *et al.*, 2013; Rhangani, 2014 and Raouf, 2019). Earliest stable fixation and anatomical reconstruction of the fracture are vital for restoration of functional ability of the injured leg. Internal fixation provides superior outcome as compared with closed methods by providing stability that allows early mobilization (Aithal *et al*., 1999 and Rathnadiwakara *et al*., 2020).

Augmenting the healing and regeneration of bone by means of tissue engineering as a part of treatment for repairing of fractures has attracted much interest among orthopaedic surgeons. Current research is focusing on the use of biomaterials to hasten fracture healing process while decreasing the time required for hospitalization, and simultaneously helping in early ambulation of the patient. The need for proper material to repair defects in bone fracture led to the advent of graft material including allografts and autografts, however immune rejection, inflammation, infection, pain, and limited availability of the graft material posed a challenge in using these graft materials (Zhang *et al.*, 2011).

Various biomaterials that were used for the augmentation of bone healing process in dogs were polymers, bioceramics, magnesium based biodegradable material and alloys. Bioceramics include tricalcium phosphate, hydroxyapatite and dicalcium phosphates (Zhang *et al*., 2011; Sheikh *et al*., 2015; Velasco *et al*., 2015; Haugen *et al*., 2019 and Filho *et al.*, 2019). Among these biomaterials, Hydroxyapatite (HA) is the most commonly used bone allograft material as it is the principal inorganic constituent of bone, and is very closely associated with the bony apatite structure. Microporosity of HA allows body fluid circulation whereas macroporosity provides scaffold for bone cell colonization which accelerates bone formation (Kilic *et al.* 1997; Paulo *et al.*, 2007; Schindler *et al*., 2008; Shayesteh *et al.*, 2008; Gibson *et al*., 2015; Kattimani *et al.*, 2016; Filho *et al.*, 2019 and Funda *et al*., 2020).

II. MATERIAL AND METHODS

The study was conducted on dogs presented to Department of Veterinary Clinical Complex College of Veterinary Science, Sri Venkateswara Veterinary University, Tirupati with long bone fractures in dogs. None of the dogs exhibited any neurological deficit, and all the dogs were presented with closed fractures. The dogs presented were 4 males and 2 females with age group ranging

International Journal of Current Science Research and Review
ISSN: 2581-8341
Volume 07 Issue 10 October 2024
DOI: 10.47191/ijcsrr/V7-i10-20, Impact Factor: 7.943
IJCSRR @ 2024
www.ijcsrr.org

from 12 months to 72 months of different breeds (2 Labrador Retriever, 1 Spitz, 1 Beagle, 1 Pug and 1 Mudhol hound).

Commercially available synthetic nanohydroxyapatite 0.5 CC was used as graft material in the study. Scanning electron microscope was used for the measurement of particle size of nanohydroxyapatite used in the study. The particle size was found to be in between 34.16 nm and 94.74 nm (fig.1).

On the day of surgery, the dogs were premedicated using atropine sulphate at the dose rate of 0.02 mg/kg body weight subcutaneously half an hour before the induction of anaesthesia. General anesthesia was induced using a combination of midazolam at a dose rate of 0.1 mg/kg body weight and ketamine hydrochloride at a dose rate of 5 mg/kg body weight administered intravenously. General anaesthesia was maintained with 2 - 3 %. Isoflurane in oxygen administered through cuffed endotracheal tube connected to circle system of small animal anesthetic machine (Boyle's anesthetic machine). Inj.Cefotaxime was administered was administered IV intra operatively at a dose rate of 20 mg/kg body weight. For all the dogs, food was withheld for 12 hours before surgery and water was provided until four hours prior to surgery.

In cases involving fractures of femur and radius-ulna the animal was placed in lateral recumbency with the affected limb placed uppermost. A cranio-lateral incision was made and extended from the level of greater trochanter to the level of patella to approach femur. The subcutaneous fat and superficial fascia were incised directly under the skin incision. Superficial leaf of the fascia lata was incised along the cranial border of the biceps femoris and the incision was extended cranially. Caudal retraction of biceps femoris revealed the shaft of femur. The fascial aponeurotic septum on the lateral shaft of bone was incised to adequately retract the vastus lateralis. For normograde pinning pin was inserted from the trochanteric fossa. Tip of the pin was secured in the craniolateral aspect of the fossa and inserted into the proximal segment. When the tip of pin is observed at the fracture site, the fracture is reduced and the pin is advanced and seated in the distal segment.

0.5 CC of nanohydroxyapatite was applied locally at the fracture site just before closing the first suture line. The tensor fascia lata was opposed with No.2-0 Polyglycolic Acid in a simple continuous pattern. Subcuticular sutures were applied in continuous pattern using No.2-0 Polyglycolic Acid. Skin was opposed with No.1-0 nylon in a cross-mattress pattern.

The skin incision is centered over the lateral edge of the radius starting near the radial head and extending to the distal end of the bone to approach radius. Subcutaneous fascia was incised on the same line as skin. The deep ante-brachial fascia was incised between the extensor carpi radialis and pronator muscles. The extensor carpi muscle was retracted cranially and the common digital extensor caudally. This exposed the body of radius and the long abductor muscle of the digit. For additional exposure of the radial shaft, flexor carpi radialis and deep digital flexor muscles were elevated caudally. The pin was placed in normograde manner, the pin was inserted between the tendons of the extensor carpi radialis and the common digital extensor on the cranial surface of the distal radius just proximal to the articular cartilage. A pilot hole was made with a pin a size smaller than selected pin. With the carpus flexed, the pin tip was started into the bone in a cranial to caudal direction. The pin angle was changed to more closely parallel to the radius as the pin was driven into the medullary canal. Once pilot hole was made, the smaller pin was removed and correct sized pin was inserted until flush with the fracture line. When the tip of pin was observed at the fracture site, the fracture is reduced and the pin is advanced and seated in the distal segment. The end of the pin was cut off and seated flush with bone so as not to interfere with the carpus. 0.5 CC of nanohydroxyapatite was applied locally at the fracture site just before closing the first suture line. The extensor muscle was opposed with No.2-0 Polyglycolic Acid in a simple continuous pattern. Subcuticular sutures were applied in continuous pattern using No.2-0 Polyglycolic Acid. Skin was opposed with No.1-0 nylon in a cross-mattress pattern.

A. Clinical signs

All six dogs presented for treatment of long bone fractures exhibited pain or localized tenderness and lameness immediately after the injury. Local swelling, non-weight bearing lameness (grade V) and abnormal angulation of limb at the fracture site and loss of function was noticed. Crepitus was observed at the fracture site on physical examination. None of the dogs exhibited any neurological deficit, and all the dogs were presented with closed fractures (fig.2). Pre-operative survey radiographs taken in all the six dogs helped to determine the fracture configuration, classify fractures and to plan the fixation procedure (fig.3).

Based on the pre-operative radiographs the fractures were classified according to AO/ASIF and the details are presented in table.1

III.RESULTS

The selected six dogs were presented with long bone fractures free from concurrent neurological, metabolic or infectious diseases were selected for this study. The fractures was stabilized using intramedullary pinning and synthetic nanohydroxyapatite

International Journal of Current Science Research and Review
ISSN: 2581-8341
Volume 07 Issue 10 October 2024
DOI: 10.47191/ijcsrr/V7-i10-20, Impact Factor: 7.943
IJCSRR @ 2024
www.ijcsrr.org

was deposited at the fracture site intra-operatively.

A. Radiographic evaluation

Follow up radiographs were evaluated on 7th, 15th, 30thand 45th post-operative days. Immediate post- operative radiographs revealed satisfactory fracture reduction to the near normal anatomical position with good cortical contact in all the cases. Immobilization was considered satisfactory in all the cases. Pin position was appropriate in all the cases. Pin length, size and position were considered appropriate in all the cases. Radiographs revealed stable implants and fracture fragments in all the cases. nanohydroxyapatite deposited at the fracture site is also visible as a radiopaque material on survey radiographs on immediate post-operative radiographs (fig.4).

The 7th day post-operative radiographs revealed that the implants were stable and fracture fragments were in apposition. Initiation of periosteal callus was evident at the fracture and indistinct fracture line was visible (fig.5) and periosteal bridging was seen (fig.6) in all the cases. Widening of the fracture gap (figs. 7 and 8) was observed by the 7th post-operative day. Nanohydroxyapatite graft material was seen near the fracture site on the survey radiographs (figs.9 and 10).

The 15th day post-operative radiographs revealed that the implants were stable and fracture fragments were in apposition. Initiation of early callus formation in the form of periosteal reaction was seen in all the cases indicative of the process of fracture healing. Unstructured patchy mineralization was seen (figs. 11 and 12) and periosteal bridging was evident in all the cases (fig.13). The fracture line was visible in all the cases except in one case where it was barely visible (fig.14 and 15). 30th day post-operative radiographs revealed that the implants were insitu and stable without any migration. Moderate bridging callus of even density with smooth borders and barely visible fracture line was seen in all the cases (fig.16). The 45th day post-operative radiographs revealed that the implants were insitu and stable. Marked bridging of the fracture site with dense callus and a barely visible fracture line complete cortical and medullary continuity was seen in all the cases (figs. 17, 18 and 19) suggestive of complete radiographic union. Early corticomedullary remodeling was evident on the radiographs in all the cases (fig.20).

Excellent weight bearing was observed in all cases (fig. 21). Complete fracture healing was observed in all the six animals with good cortical and medullary continuity with no evidence of fracture line that was suggestive of complete radiographic union and showing no signs of lameness.

B. Post operative care and management

The animals were kept under observation on the floor in a well-ventilated room with neck in extended position and movement restricted until complete recovery from anesthesia. Immediate post-operative radiographs in cranio-caudal and medio-lateral views were taken. Post-operatively, the operated limb was supported by Modified Robert-Jones bandaging after antiseptic dressing using 5 % povidone-iodine. The bandage was changed on alternate days until suture removal. Post-operatively, all the dogs were administered broad spectrum antibiotic Inj. Cefotaxime @ 20 mg/kg body weight, IM, twice daily for 7 days. Analgesia was provided by Inj. Meloxicam[2] @ 0.3 mg/kg body weight, IM, once a day for 3 days. Osteopet[3] was given orally twice daily for 30 days. Skin sutures were removed after 10 days of surgery. Restricted movement was advised for the first 10 days followed by leash walking. Physiotherapy of the limb i.e., flexion and extension of carpal joint, stifle joint and tarsal joint was advised thrice daily to retain normal joint movement from 14th post- operative day up to 6-8 weeks till normal joint mobility was seen.

C. Wound healing

The skin suture line healed by first intention healing in all the dogs (n=6). The incisional wound healed without any complications in all the cases. The open wounds in the cases were healed by the end of 7th post-operative day.

D. Weight bearing and angulation

Post-operative weight bearing on the operated limb of the dogs was assessed while standing and walking. Angulation of the limb was assessed clinically by comparing the conformation of the affected limb and the position of the paw with the contra-lateral limb while standing. Initial weight bearing on the operated limb was recorded as early as on 2nd post-operative day in all the cases (n=6). The mean initial weight bearing time was 2.5 ± 0.22 days. Most of the dogs had partial weight bearing with paw touching on the ground by the end of first post-operative day, while complete weight bearing was observed by the 2nd and 3rd post- operative days.

International Journal of Current Science Research and Review
ISSN: 2581-8341
Volume 07 Issue 10 October 2024
DOI: 10.47191/ijcsrr/V7-i10-20, Impact Factor: 7.943
IJCSRR @ 2024
www.ijcsrr.org

E. Implant removal

Implant removal was carried out in all the animals based on satisfactory functional outcome and radiological confirmation of bony union**.** Out of the total 6 cases, implants were removed in 2 animals after complete radiographic union was evident. At the time of removal of implant complete radiographic union was evident with minimal callus formation and continuity of the medullary canal. (figs. 22, 23, 24 and 25).

IV. CONCLUSION

Nanohydroxyapatite with intramedullary pinning enabled achievement of a stable and reliable fixation of fractures of long bones in dogs and resulted in early limb ambulation and excellent healing as evidenced by the clinical outcome.

V. ACKNOWLEDGEMENTS

The authors thank the authority of Sri Venkateswara Veterinary University for providing the necessary infrastructure for conducting the research work.

REFERENCES

1. Aithal, H. P., Singh, G. R., Amarpal., Kinjavdekar, P., and Setia, H. C. 1999 Fractures secondary to nutritional bone disease in dogs: a review of 38 cases. Journal of Veterinary Medicine Series, A. 46 (8): 483-487.
2. Ali, L. B. 2013 Incidence, occurrence, classification, and outcome of small animal fractures: a retrospective study (2005-2010). *0*, 7 (3): 191-196.
3. Filho, B. M., and Medrado, A. R. 2019 Biological principles of nanostructured hydroxyapatite associated with metals: a literature review. Insight Biomed, 4 (3), 1-10.
4. Sheikh, Z., Najeeb, S., Khurshid, Z., Verma, V., Rashid, H., and Glagauer, M. 2015 Biodegradable materials for bone repair and tissue engineering applications. Materials, 8.9: 5744-5794.
5. Haugen, H. J., Lyngstadaas, S. P., Rossi, F., and Perale, G. 2019 Bone grafts: which is the ideal biomaterial?. Journal of Clinical Periodontology, 46: 92-102.
6. Kumar, K., Mogha, I. V., Aithal, H. P., Kinjavdekar, P., Amarpal., Singh, G. R., Pawde, A. M., and Kushwaha, R. B. Occurrence and pattern of long bone fractures in growing dogs with normal and osteopenic bones. Journal of Veterinary Medicine Series *A* 54.9 (2007): 484-490.
7. Kushwaha, R. B., Gupta, A. K., Bhadwal, M. S., Kumar, S., and Tripathi, A. K. 2011 Incidence of fractures and their management in animals: a clinical study of 77 cases. Indian Journal of Veterinary Surgery 32: 54-56.
8. Raouf, M., Ezzeldein, S. A., and Eisa, E. F. M. 2019 Bone fractures in dogs: A retrospective study of 129 dogs. Iraqi Journal of Veterinary Sciences, 33(2): 401-40.
9. Ratnadiwakara, R. W. M. H., Silva, D. D. N., and Wijekoon, H. M. S. 2020 Treatment of supracondylar femoral fractures in young cats and dogs using “Arrow Pin” technique. Journal of Veterinary Animal Science. 3(1): 1017.
10. Rhangani, A. T. 2014 Incidence, classification, and management of appendicular bonefractures in dogs in Nairobi County, Kenya. A retrospective study. Doctoral Dissertation University of Nairobi, pp. 22-31.
11. Simon, S. M. Ganesh, R., Ayyappan, S., and Kumar, S. R. 2011 Incidence of pectoral limb fractures in dogs: a survey of 331 cases. Tamilnadu Journal of Veterinary Animal Science, 7.2: 94-96.
12. Şirin, O. S., Kaya, U., and Olcay, B. 2013 Clinical and radiological outcomes of locking compression plate system in dogs with diaphyseal fractures: 32 cases. The Journal of the Faculty of Veterinary Medicine, 19: A13-A18.
13. Velasco, M. A., Narvaez, A., Tovar, C. A., and Alvarado, D. A. 2015 Design, materials, and mechanobiology of biodegradable scaffolds for bone tissue engineering. BioMed research international, 2015.
14. Zhang, Z. G., Li, Z. H., Mao, X. Z., and Wang, W. C. 2011 Advances in bone repair with nano biomaterials: mini- review. Cytotechnology, 63(5): 437.

International Journal of Current Science Research and Review
ISSN: 2581-8341
Volume 07 Issue 10 October 2024
DOI: 10.47191/ijcsrr/V7-i10-20, Impact Factor: 7.943
IJCSRR @ 2024
www.ijcsrr.org

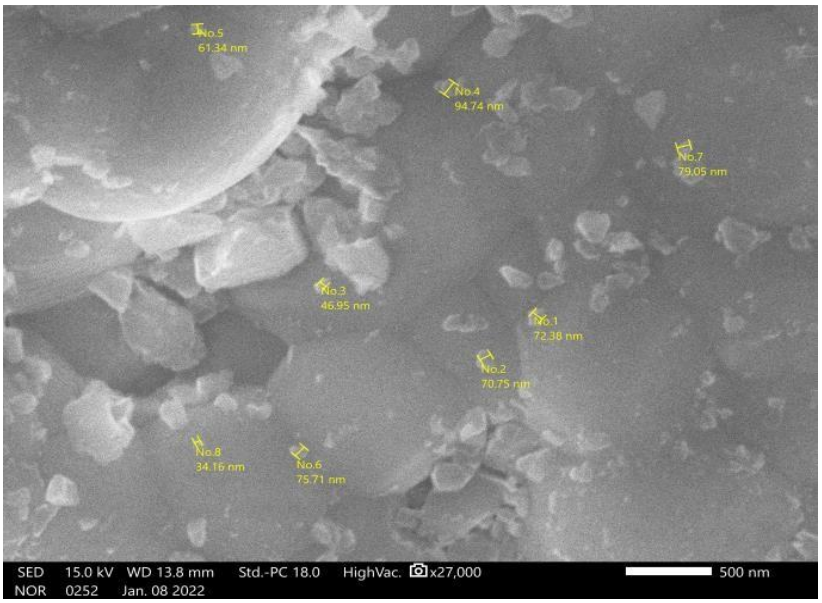

Fig. 1. Scanning electron microscope picture of nanohydroxyapatite (HA NANO, B-OSTIN, Basic Health care, Baddi, Himachal Pradesh, India) used in the study


Dog-1


Dog-2


Dog-3


Dog-4


Dog-5


Dog-6

Fig. 2. Pre-operative photographs showing grade V lameness

International Journal of Current Science Research and Review
ISSN: 2581-8341
Volume 07 Issue 10 October 2024
DOI: 10.47191/ijcsrr/V7-i10-20, Impact Factor: 7.943
IJCSRR @ 2024
www.ijcsrr.org

Dog-1-33C3 Dog-2-32A3 Dog-3-33A3

Dog-4-32B3 Dog-5-32C3 Dog-6-23A3

Fig. 3. Pre-operative survey radiographs

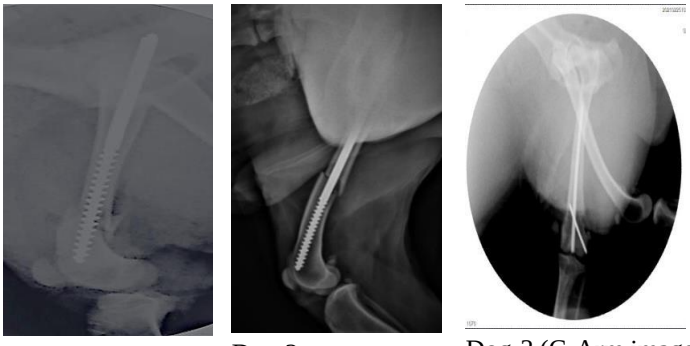

Dog-1 Dog-2 Dog-3 (C-Arm image)

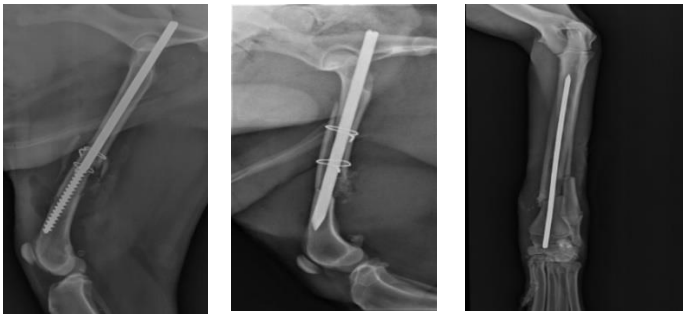

Dog-4 Dog-5 Dog-6

Fig. 4. Immediate post-operative radiographs showing long bone fractures

International Journal of Current Science Research and Review
ISSN: 2581-8341
Volume 07 Issue 10 October 2024
DOI: 10.47191/ijcsrr/V7-i10-20, Impact Factor: 7.943
IJCSRR @ 2024
www.ijcsrr.org

Fig. 5. 7th post-operative day Medio- lateral radiograph showing indistinct fracture margins in dog 1

Fig. 6. 7th post-operative day Cranio- caudal radiograph showing indistinct fracture margins with periosteal bridging in dog 1

Fig. 7. 7th post-operative day Medio- lateral radiograph showing widening of fracture gap in dog 5

Fig. 8. 7th day cranio-caudal radiograph showing widening of fracture margins in dog 5

Fig. 9. 7th day medio-lateral radiograph showing graft at the fracture site in dog 6

Fig. 10. 7th day cranio-caudal radiograph showing graft material at the fracture site with in dog 6

Fig. 11. 15th day medio-lateral radiograph showing unstructured patchy mineralization of bridging callus and evident fracture line in dog 1

Fig. 12. 15th day medio-lateral radiograph showing patchy mineralization of bridging callus in dog 5

Fig. 13. 15th day cranio-caudal radiograph showing periosteal bridging in dog 1

International Journal of Current Science Research and Review
ISSN: 2581-8341
Volume 07 Issue 10 October 2024
DOI: 10.47191/ijcsrr/V7-i10-20, Impact Factor: 7.943
IJCSRR @ 2024
www.ijcsrr.org

Fig. 14. 15th day medio-lateral radiograph showing bridging callus with even density and barely visible fracture line in dog 6

15. 15th day cranio-caudal radiograph showing barely visible fracture line and patchy mineralization of bridging callus in dog 6

Fig. 16. 30th day medio-lateral radiograph showing bridging callus of even density and smooth bordering with barely visible fracture line in dog 6

Fig. 17. 45th day medio-lateral radiograph showing early corticomedullary remodeling in dog 1

International Journal of Current Science Research and Review
ISSN: 2581-8341
Volume 07 Issue 10 October 2024
DOI: 10.47191/ijcsrr/V7-i10-20, Impact Factor: 7.943
IJCSRR @ 2024
www.ijcsrr.org

Fig. 18. 45th day cranio-caudal radiograph showing dense callus and barely visible fracture line in dog 1

Fig. 19. 45th day cranio-caudal radiograph showing dense callus and barely visible fracture line in dog 6

Fig. 20. 45th day medio-lateral radiograph showing early corticomedullary remodeling in dog 6

Fig. 21. Showing complete weight bearing by 2nd post-operative day in dog 6

International Journal of Current Science Research and Review
ISSN: 2581-8341
Volume 07 Issue 10 October 2024
DOI: 10.47191/ijcsrr/V7-i10-20, Impact Factor: 7.943
IJCSRR @ 2024
www.ijcsrr.org

Fig. 22. 75th day post-operative radiograph showing dense callus with corticomedullary separation and complete cortical continuity of dog 1

Fig. 23. 75th day post-operative radiograph after implant removal showing corticomedullary separation and complete cortical continuity of dog 1

Fig. 24. 80th post-operative radiograph showing dense callus of reduced size in dog 6

International Journal of Current Science Research and Review
ISSN: 2581-8341
Volume 07 Issue 10 October 2024
DOI: 10.47191/ijcsrr/V7-i10-20, Impact Factor: 7.943
IJCSRR @ 2024
www.ijcsrr.org

Fig. 25. 80th post-operative radiograph showing condensation of callus, indistinct corticomedullary remodelling with complete cortical continuity of dog 6

Table.1.AO/ASIF Classification of long bone fractures

Sr.No	AO/ASIF Classification	Type Of Fracture
1	33C3	Complete, distal third, comminuted, moderately overriding, angularly displaced femur fracture
2	32A3	Complete, mid-shaft, transverse, mildly overriding femur fracture
3	33A3	Complete, distal metaphyseal, transverse, displaced femur fracture
4	32B3	Complete, mid-shaft, comminuted, mildly overriding, femur fracture with a reducible wedge on cranial aspect of fracture
5	32C3	Complete, mid-shaft, comminuted, moderately overriding femur fracture with multiple wedges at fracture site
6	23A3	Complete, distal third, oblique, mildly overriding fracture of radius-ulna

Cite this Article: E Sony Sharlet, S Bharathi, R V Suresh kumar, M Santhilakshmi (2024). A Clinical and Radiographical Study on Augmentation of Fracture Healing in Long Bones of Dogs Using Synthetic Nanohydroxyapatite. International Journal of Current Science Research and Review, 7(10), 7654-7664, DOI: https://doi.org/10.47191/ijcsrr/V7-i10-20